0013-7227/99/$03.00/0
Endocrinology

Vol. 140, No. 12
Printed in U.S.A.

Generation of Antisera to Mouse Insulin-Like Growth Factor Binding Proteins (IGFBP)-1 to -6: Comparison of IGFBP Protein and Messenger Ribonucleic Acid Localization in the Mouse Embryo*

M. VAN KLEFFENS, C. A. H. GROFFEN, N. F. J. DITS, D. J. LINDENBERGH-KORTLEVE, A. G. P. SCHULLER, S. L. BRADSHAW, J. E. PINTAR, E. C. ZWARTHOFF, S. L. S. DROP, AND J. W. VAN NECK

Laboratory of Pediatrics (M.v.K., C.A.H.G., N.F.J.D., D.J.L.-K., S.L.S.D., J.W.v.N.), Subdivision Molecular Endocrinology, and Department of Pathology (E.C.Z.), Erasmus University Rotterdam, Postbus 1738, 3000 DR Rotterdam, The Netherlands; and Department of Neuroscience and Cell Biology (A.G.P.S., S.L.B., J.E.P.), University of Medicine and Dentistry of New Jersey, Robert Wood Johnson Medical School, Piscataway, New Jersey 08854

ABSTRACT

The insulin-like growth factor (IGF) system is an important regulator of fetal growth and differentiation. IGF bioavailability is modulated by IGF binding proteins (IGFBPs). We have generated six different antisera, directed to synthetic peptide fragments of mouse IGFBP-1 through -6. The specificity of the produced antisera was demonstrated by enzyme-linked immunosorbent assay, Western blotting, and by immunohistochemistry on sections of mouse embryos of 13.5 days post coitum. Specificity for the IGFBP-2 through -6 antisera also was confirmed immunohistochemically in liver and lung of corresponding gene deletion (knock-out) mutant mice and wild-type litter mates.

Immunohistochemistry and messenger RNA (mRNA) *in situ* hybridization on sections of mouse embryos of 13.5 days post coitum revealed tissue-specific expression patterns for the six IGFBPs. The only site of IGFBP-1 protein and mRNA production was the liver. IGFBP-2, -4, and -5 protein and mRNA were detected in various organs and tissues. IGFBP-3 and -6 protein and mRNA levels were low. In several tissues, such as lung, liver, kidney, and tongue, more than one IGFBP (protein and mRNA) could be detected. Differences between mRNA and protein localization were extensive for IGFBP-3, -5, and -6, suggesting that these IGFBPs are secreted and transported.

These results confirm the different spatial localization of the IGFBPs, on the mRNA and protein level. The overlapping mRNA and protein localization for IGFBP-2 and -4, on the other hand, may indicate that these IGFBPs also function in an auto- or paracrine manner. (*Endocrinology* **140:** 5944–5952, 1999)

THE INSULIN-LIKE growth factor (IGF) binding proteins (IGFBPs) are a family of at least six highly homologous proteins that bind IGF with high affinity (1). Together with the IGF receptors, IGFs and IGFBPs form the IGF system that is important during development, where IGFBPs serve as regulators of IGF bioavailability (2–5). Human fetal tissues synthesize and secrete IGFBPs in a tissue-specific fashion (6–9).

Mouse models are widely used to obtain insight into the actions of the IGF system members during development (10–14). Gene expression studies have shown that the IGF system components have specific spatial and temporal messenger RNA (mRNA) expression patterns during development (15–20). Because the IGFs and IGFBPs are secreted proteins, it is relevant to extend analysis of gene transcription to the localization of the proteins at their site of action.

Received March 1, 1999.

Address all correspondence and requests for reprints to: Dr. J. W. van Neck, Erasmus University Rotterdam, Laboratory of Pediatrics, Room Ee15.00, Postbus 1738, 3000 DR Rotterdam, The Netherlands. E-mail: vanneck@kgk.fgg.eur.nl.

* This project was supported by grants from the Netherlands Organization for Scientific Research (Grant 901–28-088, to J.W.v.N.; and grant S-91-245, to A.G.P.S.), the Sophia Foundation for Medical Research (to D.J.L.-K. and J.W.v.N.), the Lalor Foundation (to A.G.P.S. and S.L.B.), and NIH Grant NS-21970 (to J.E.P.).

Several studies have confirmed the tissue-specific protein localization of the components of the IGF system in the human (7–9). The existing antibodies to rat IGFBPs, however, are not applicable in immunohistochemical detection in mice (21).

Therefore, the aim of this study was to generate specific antisera against the mouse IGFBPs (mIGFBPs) and to compare IGFBP protein localization patterns with IGFBP mRNA patterns during mouse development. Specific mIGFBP antisera were raised using synthetic peptides specific for each of the IGFBPs and were characterized by enzyme-linked immunosorbent assay (ELISA), Western blotting, and immunohistochemistry. Immunohistochemistry and *in situ* hybridization were performed on sections of 13.5-dpc (days post coitum) mouse embryos to analyze protein and mRNA localization of the six IGFBPs.

Materials and Methods

Generation of antisera

Antisera to mIGFBP-1, -2, -3, -4, -5, and -6 were generated using synthetic peptides (ID-DLO, Lelystad, The Netherlands) (Table 1). These peptides were chosen from the unique middle part of the IGFBP amino acid sequences, to limit cross-reactivity between the various IGFBPs. The choice of the peptide fragments was guided by hydrophobicity plots (22), surface probability predictions according to Emini, Chou-Fasman

TABLE 1. Amino acid sequences of the synthetic peptide fragments of the IGFBPs used to produce anti-mIGFBP antisera

IGFBP-1	^{174}MRAREIADLKKWKEPC^{189}
IGFBP-2	^{173}CEKVNEQHRQMGKGAKH^{189}
IGFBP-3	^{200}FSSESKRETEYGPC^{213}
IGFBP-4	^{155}VGTPREEPRPVPQGSC^{170}
IGFBP-5	^{177}VIPAPEMRQESEQGPC^{192}
IGFBP-6	^{127}CSRDTNHRDRQKNPRTS^{143}

The amino acid numbering of the corresponding IGFBP fragment are given above.

secondary structure predictions (23), and antigenicity index (24). A terminal cystein was added to the peptide for sulfhydryl coupling. Conjugation to the carrier keyhole limpet hemocyanin (KLH) was performed, following the manufacturer's prescription (Pierce Chemical Co., Rockford, IL). KLH-coupled peptides were injected sc into rabbits (0.25 mg), using specol (Central Veterinary Institute, Lelystad, the Netherlands) as adjuvant. Three weeks after primary immunization, the rabbits were boosted (protocol similar to primary immunization). After a final boost, 3 weeks later (similar to previous boost), sera were collected and used in subsequent experiments.

ELISA

A total of 96 microwell plates were coated with peptide (without KLH), 2 μg/ml in coupling buffer (50 mM carbonate buffer, pH 9.0), and dried overnight at 37 C. After blocking with 3% BSA (fraction V; Roche Molecular Biochemicals GmbH, Mannheim, Germany) in PBS dilution gradients of the antisera were pipetted into the wells (1:500 to 1:16,000), which were incubated overnight at 4 C. A peroxidase-conjugated swine antirabbit antibody (DAKO Corp., Glostrup, Denmark) was used as a secondary step (dilution 1:1,000) during 1 h. Detection was done with o-phenyl diamine (Eastman Kodak Co., Rochester, NY) (20 mg o-phenyl diamine + 50 μl H_2O_2/10 ml 0.1 M citric acid, 0.2 M Na_2HPO_4, pH 5.0). The reaction was stopped with 5 M H_2SO_4.

Negative controls were included, consisting of incubation of the wells plate, coated with peptides, with preimmune sera of the respective antisera, in the same dilutions. Cross-reactivity was checked by incubating each peptide with all IGFBP antisera (dilutions 1:500 and 1:1,000).

Western blotting

Murine erythroleukemia (MEL) cells were transfected with IGFBP-1, 2, 4, and 6 complementary DNAs (17), according to Needham and co-workers (25). In the log phase, these cells were induced for 48 h with dimethylsulfoxide. Subsequently, cell culture medium was trichloric acid precipitated (50 vol/vol 20%trichloric acid, overnight at 4 C) (Merck KGaA, Darmstadt, Germany). IGFBP production was tested by IGF-ligand blotting, as described by Hossenlopp *et al.* (26).

For IGFBP-3, normal mouse serum was used; whereas for IGFBP-5, total protein was extracted from fetal mouse lungs (13.5 dpc) by the TRIzol method, following the manufacturer's prescription (Life Technologies, Rockville, MD).

Proteins were separated on a reducing 8% or 10% SDS:PAGE and transferred either to polyvinylidene difluoride (PVDF) (Millipore Corp., Bedford, MA) or nitrocellulose (Schleicher & Schuell, Inc., Dassel, Germany) membranes. The PVDF membranes were blocked with 5% nonfat dry milk (Profilar, Nutricia, Zoetermeer, the Netherlands), the nitrocellulose membranes with 3% BSA (Roche Molecular Biochemicals GmbH). Membranes were incubated overnight at 4 C with the primary antibody (dilutions varying from 1:200 to 1:20,000). As a secondary step, a peroxidase-conjugated swine antirabbit antibody was used (DAKO Corp., A/S; 1:2,000) on the PVDF membranes, 1 h at room temperature. The nitrocellulose membranes were incubated with a secondary alkaline phosphatase antibody (DAKO Corp., A/S). PVDF membranes were incubated according to the manufacturer's procedure (Pierce Chemical Co.) and subsequently covered with ECL hyperfilms (Amersham Pharmacia Biotech, Buckinghamshire, UK). Films were illuminated varying from 1 min to 2 h, depending on the intensity of the signal. Detection on nitrocellulose membranes took place with NBT (4-nitroblue tetrazolium chloride) and BCIP (5-bromo-4-chloro-3-indolyl-phosphate).

Immunohistochemistry on sections

Balb/c mice were mated, and the morning of appearance of a vaginal plug was assigned 0.5 dpc. Pregnant females were killed by cervical dislocation, and embryos were collected at 13.5 dpc and fixed overnight in 4% paraformaldehyde. Similarly, liver and kidneys from adult gene deletion (knock-out) IGFBP-2 through -6 mutants (27–30) and their wild-type litter mates were fixed overnight in 4% paraformaldehyde. After embedding of the fixed tissues in paraffin, 5-μm sections were cut and mounted onto aminopropyl trioxysilane-coated slides. Immunohistochemistry was performed, making use of a peroxidase-antiperoxidase (PAP) method or an avidine-biotine complex method. The anti-mIGFBP antisera were used in a dilution of 1:250. Unlabeled goat antirabbit Igs (dilution 1:50) (DAKO Corp.) were used as second antibody and rabbit PAP (dilution 1:100) (DAKO Corp.) as a linker in the PAP method. Incubation with a biotin-conjugated goat antirabbit (DAKO Corp.), completed with a streptavidin horseradish peroxidase complex (BioGenex Laboratories, Inc., San Ramon, CA) incubation, was used for the avidine-biotine complex method. Staining was performed with diaminobenzidine (0.75 mg/ml) (DAB, Fluka Chemical Co., Buchs, Switzerland). Nuclei were visualized with Mayer's hematoxilin. The tissues were analyzed under light microscopy. Controls were performed on sections with preimmune sera of each rabbit, diluted 1:10 to 1:50. As a second control, the immune sera were mixed in a dilution range with the corresponding peptides (1, 0.5, and 0.17 μg/μl) and incubated overnight at 4 C. With these mixtures, immunohistochemistry on sections of mouse embryos was performed.

Probe preparation (in situ hybridization)

Specific mIGFBP complementary RNA probes were transcribed from IGFBP-2, -3, -4, -5, and -6, as described by Schuller *et al.* (17). The mouse complementary DNA *Sph*I-*Sac*I fragment was used as template for the IGFBP-1 complementary RNA probe and was cloned into pTZ18R or pTZ19R (Amersham Pharmacia Biotech, Uppsala, Sweden) for the antisense and sense probes, respectively. Digoxigenin-11-UTP-labeled RNA probes were prepared according to the manufacturer's prescription (Roche Molecular Biochemicals GmbH) using T7 or SP6 RNA polymerase.

In situ hybridization

A nonradioactive *in situ* hybridization was performed, essentially as described before (16). Hybridization was performed overnight at 55 C in a humid chamber in a hybridization solution containing 50% deionized formamide, 10% dextran sulfate, 2 × SSC, 1 × Denhardt's solution, 1 μg/ml transfer RNA, 250 μg/ml herring sperm DNA, and the respective probes at a concentration of 100 ng/ml. After various washes (50% formamide/2 × SSC, 50% formamide/1 × SSC, and 0.1 × SSC) sections were incubated with ribonuclease T1 (2 U/ml in 1 mM EDTA/2 × SSC) for 15 min at 37 C. The digoxigenin-labeled hybrids were detected by antibody incubation performed according to the manufacturer's recommendations (Roche Molecular Biochemicals GmbH). PVA (Polyvinylalcohol; molecular mass, 31–50 kDa; Aldrich, Milwaukee, WI)-enhanced staining with BCIP, NBT, and levamisol was stopped when the desired intensity of the blue precipitate was reached. This was dependent on the relative abundance of the respective mRNAs. Sections were counterstained with Nuclear red solution and mounted with Euparal (ChromaGesellschaft, Stuttgart, Germany). Negative controls for *in situ* hybridization were performed using sense probes, which never gave any significant staining.

Results

Analysis of antisera specificity and cross-reactivity

After immunization and boost, all rabbits developed antisera against the predicted mIGFBP. ELISA assay of the antisera demonstrated a specific response to the injected peptides (results not shown). Antisera against mIGFBP-1, -3, -4, and -6 were very specific and already demonstrated a clear color reaction at a dilution to 1:8,000. Clear color reaction of antisera against IGFBP-2 and -5 were obtained at a

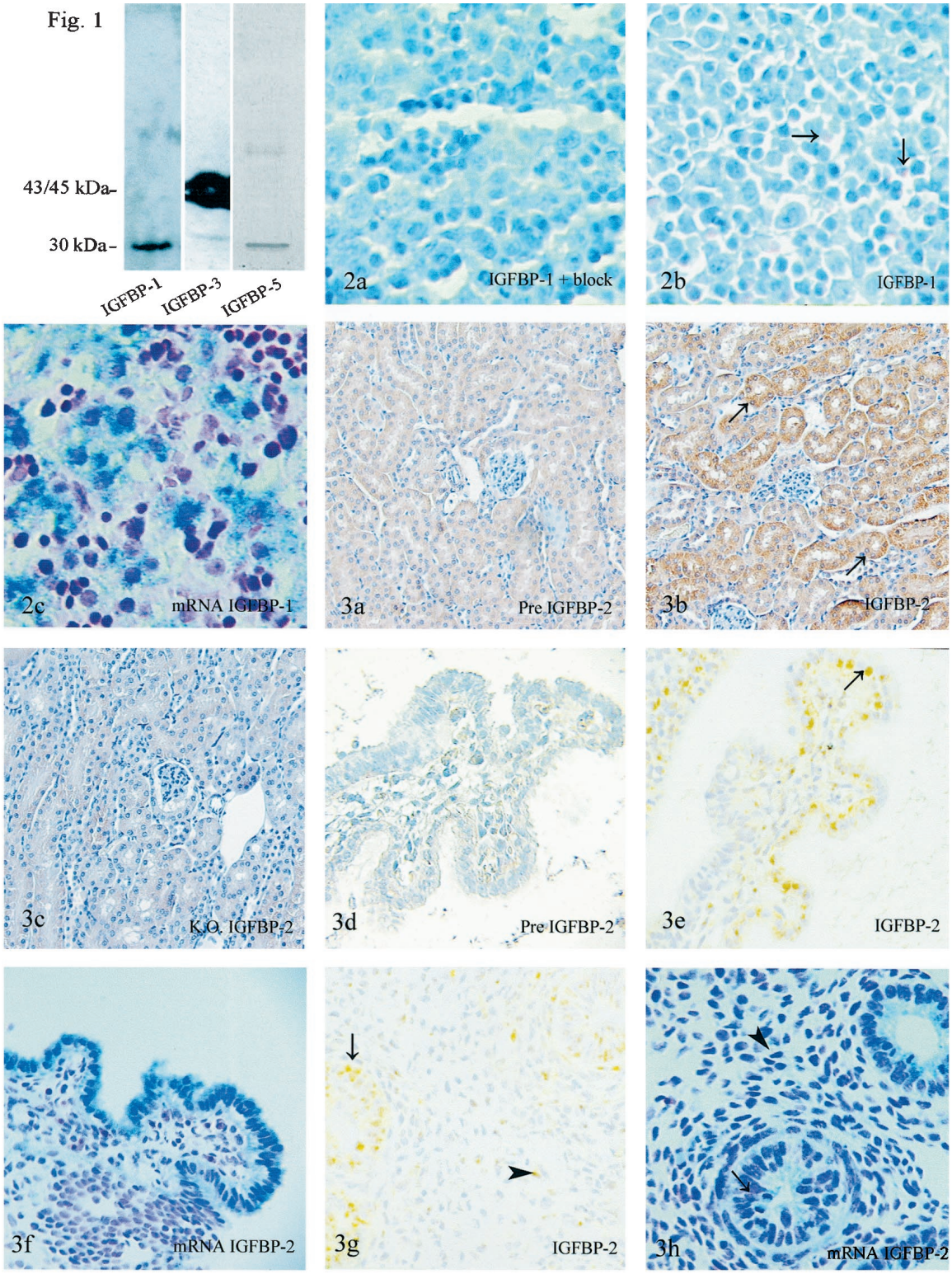

FIGS. 1–3. FIG. 1. Western immunoblots of mIGFBP-1, -3, and -5. mIGFBP-1: 100 μg IGFBP-1 containing culture supernatant from MEL cells (ECL); dilution of the mIGFBP-1 antiserum, 1:20,000. IGFBP-3: 1 μl normal mouse serum (ECL); dilution of the mIGFBP-3 antiserum, 1:10,000. IGFBP-5: total protein (80 μg) of 13.5-dpc mouse lungs (NBT/BCIP staining), dilution of the mIGFBP-5 antiserum, 1:1,000. FIG. 2. IGFBP-1 immunohistochemistry on the liver of a 13.5-dpc mouse embryo. a, Antiserum against IGFBP-1 (1:250) was blocked with 60 ng of the corresponding IGFBP-1 per slide; b, IGFBP-1 (antiserum against IGFBP-1, 1:250; *arrows*, weak immunohistochemical staining of IGFBP-1); c, IGFBP-1 mRNA (*blue*) by *in-situ* hybridization. FIG. 3. Immunohistochemical detection of IGFBP-2 protein (*brown*) and IGFBP-2 mRNA (*blue*) in mouse adult kidney (a–c) and in embryonic (13.5-dpc) choroid plexus (d–f) and lung (g and h). a, Kidney, preimmune serum (1:20) as a control for background staining; b, kidney, IGFBP-2 protein (*arrow*, IGFBP-2 protein in proximal tubules); c, kidney obtained from an IGFBP-2 gene

dilution of 1:4,000. As a control, incubation with each of the preimmune sera in a dilution range was included that showed no significant staining. No cross-reactivity between the antisera and the synthetic nonhomologous IGFBP peptide fragments was observed (data not shown).

Detection of mIGFBPs on Western blot was possible for mIGFBP-1, -3, and -5 (Fig. 1). The patterns on Western blot corresponded with the IGF-ligand blot results (data not shown). A distinct band of approximately 30 kDa was visible for mIGFBP-1, after dilution of the antiserum to 1:20,000. When 1 μl mouse serum was loaded, the IGFBP-3 43–45 kDa doublet was visible after incubation with the anti-IGFBP-3 antiserum (diluted 1:10,000). Loading of total protein of 13.5-dpc mouse lungs gave a band of approximately 29 kDa when incubated with the IGFBP-5 antiserum (1:1,000). Neither of the antisera demonstrated cross-reactivity to the other IGFBPs.

Specificity of immunohistochemical detection of IGFBPs in mouse tissues

Specificity of the generated mIGFBP antisera in immunohistochemistry was checked by incubating the antisera overnight with the corresponding synthetic peptides in a dilution range (60–10 ng/ml). Subsequently, these mixtures were used in an immunohistochemical procedure on sections of 13.5-dpc mouse embryos. This resulted in a gradual loss of signal with increasing peptide concentrations. An example is given in Fig. 2. The loss of signal did not occur when nonhomologous peptides were used (data not shown).

Furthermore, for the antisera directed against mIGFBP-2 through -6, specificity was determined, using immunohistochemistry on sections of liver and kidney from wild-type animals, using preimmune serum as a control for background staining (see panels a in Figs. 3–7), on liver and kidney from adult wild-type animals using the antiserum (see panels b in Figs. 3–7), and on livers and kidneys from adult gene deletion (knock-out) mutants with their respective antisera as a negative control (see panels c in Figs. 3–7).

IGFBP-2 preimmune serum resulted in a uniform background staining of renal structures including the tubules (Fig. 3a). The mIGFBP-2 antiserum revealed a prominent staining of the renal proximal tubules (Fig. 3b) that was absent in IGFBP-2 gene deletion mutants (Fig. 3c).

IGFBP-3 preimmune serum resulted in a weak, uniform hepatic staining (Fig. 4a). The mIGFBP-3 antiserum prominently stained the endothelium of the veins and arteries (Fig. 4b) that was absent in IGFBP-3 gene deletion mutants (Fig. 4c).

IGFBP-4 preimmune serum revealed a weak uniform hepatic staining (Fig. 5a). The mIGFBP-4 antiserum staining was located around hepatic veins (Fig. 5b) and was absent in IGFBP-4 gene deletion mutants (Fig. 5c).

IGFBP-5 preimmune serum resulted in a moderate staining of all renal tubules (Fig. 6a), whereas the mIGFBP-5 antiserum demonstrated a strong staining of the renal proximal tubules superimposed on the background staining (Fig. 6b). This was in contrast to the IGFBP-5 gene deletion mutants that only demonstrated a weak general renal staining (Fig. 6c).

IGFBP-6 preimmune serum resulted in a moderate staining of all renal structures including the tubules (Fig. 7a). The mIGFBP-6 antiserum demonstrated a strong staining of those renal proximal tubules that were located in the proximity of a blood vessel (Fig. 7b). This staining was absent in kidney obtained from IGFBP-6 gene deletion mutants (Fig. 7c).

Comparison of protein and mRNA localization of the six IGFBPs in the 13.5-dpc mouse embryo

The antisera against mIGFBP-1 through -6 were applied to paraffin sections of mouse embryos (13.5 dpc) to localize mIGFBP proteins. Similarly, mRNA expression patterns in 13.5-dpc mouse embryos were determined by *in situ* hybridization. *In situ* hybridization and immunohistochemistry staining patterns are summarized in Table 2.

IGFBP-1 gene expression was limited. Staining of IGFBP-1 protein was visualized only in the liver, similar to IGFBP-1 mRNA expression (Fig. 2, b and c).

Like IGFBP-2 mRNA expression, IGFBP-2 protein occurrence was diverse. Major sites of IGFBP-2 protein localization were liver, kidney, choroid plexus, lung, and floor plate. This is in accordance with mRNA expression. Both IGFBP-2 mRNA and protein were located in the epithelial cells of the kidney and choroid plexus (Fig. 3, d–f). In lung, IGFBP-2 mRNA and protein were present in the tubule, but also scattered in underlying mesenchymal cells (Fig. 3, g and h). However, there was a discrepancy between the tubular localization of IGFBP-2 mRNA and protein. The mRNA was located in the epithelial cells, whereas IGFBP-2 protein was detected in the underlying tubular cells.

IGFBP-3 mRNA expression was weak and colocalized with IGFBP-3 protein in liver, tongue, lung and in nose epithelium (very weak signal) (Fig. 4, d–g). In the tongue, IGFBP-3 mRNA and protein were not colocalizing but expressed in neighboring cell types in muscle (Fig. 4, f and g). In contrast to mRNA expression, IGFBP-3 protein also could be detected in the choroid plexus and kidney, whereas mRNA expression could also be detected in the heart.

In accordance with its mRNA expression, staining of IGFBP-4 protein was detected widespread. Overlapping mRNA and protein expression was visualized in mesencephalon, telencephalon (Fig. 5, d and e), heart, liver, lung, tongue mesenchyme, and blood vessels. In addition to the mRNA expression profiles, IGFBP-4 protein could be demonstrated in the kidney (results not shown).

IGFBP-5 mRNA was expressed abundantly and was largely overlapping protein occurrence. Identical to mRNA expression, IGFBP-5 protein was localized in the liver, endothelium of the gut, meninges, tubules and mesenchyme of the lung (very weak protein staining) (Fig. 6, d–g), and

deletion (K.O.) mutant, control for the specificity of the IGFBP-2 antiserum; d, choroid plexus, preimmune serum as a negative control for IGFBP-2 (1:20); e, IGFBP-2 protein in the choroid plexus (*arrows*, IGFBP-2 protein in epithelial cells); f, IGFBP-2 mRNA in the choroid plexus; g, IGFBP-2 protein in lung (*arrow*, IGFBP-2 protein in tubular cells; *arrowhead*, IGFBP-2 protein in mesenchymal cells); h, IGFBP-2 mRNA in lung (*arrow*, localization in epithelial cells; *arrowhead*, localization in mesenchymal cells).

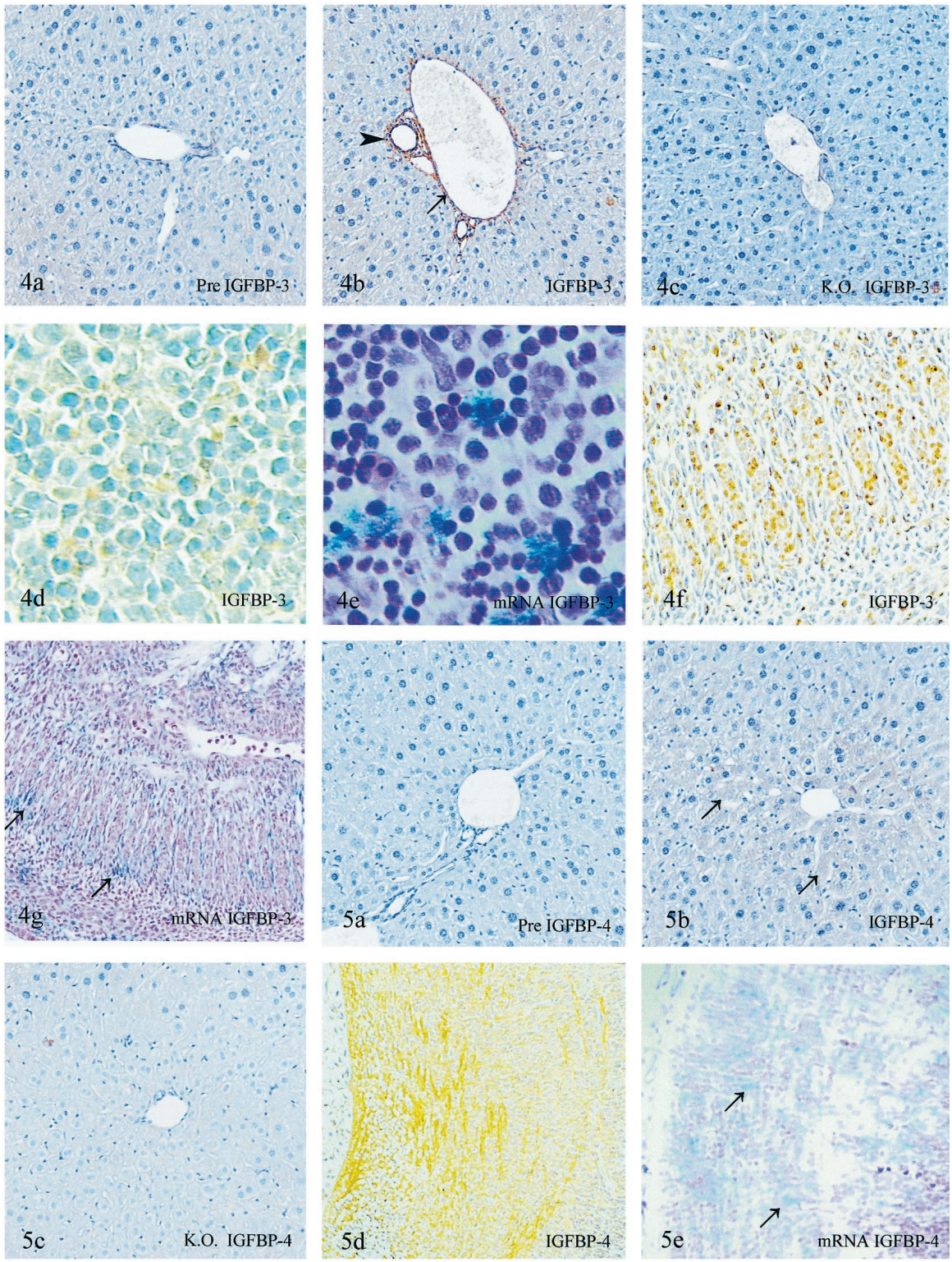

FIGS. 4–5. FIG. 4. Immunohistochemical detection of IGFBP-3 protein (*brown*) and IGFBP-3 mRNA (*blue*) in mouse adult liver (a–c) and in embryonic (13.5-dpc) liver (d and e) and tongue (f and g). a, Liver, serum (1:20) as a control for background staining; b, liver, IGFBP-3 protein (*arrow*, IGFBP-3 protein in venous endothelium; arrowhead, IGFBP-3 protein in a hepatic artery; c, liver obtained from an IGFBP-3 gene deletion (K.O.) mutant, control for the specificity of the IGFBP-3 antiserum; d, IGFBP-3 protein in liver; e, IGFBP-3 mRNA in liver; f, IGFBP-3 protein in tongue (muscle); g, IGFBP-3 mRNA (*arrow*) neighbors IGFBP-3 protein in tongue. FIG. 5. Immunohistochemical detection of IGFBP-4 protein (*brown*) and IGFBP-4 mRNA (*blue*) in mouse adult liver (a–c) and in 13.5-dpc embryonic hindbrain (d and e). a, Liver, preimmune serum (1:20) as a control for background staining; b, IGFBP-4 protein (*arrow*, IGFBP-4 protein in cells surrounding a hepatic vein); c, liver obtained from an IGFBP-4 gene deletion (K.O.) mutant, control for the specificity of the IGFBP-4 antiserum; d, IGFBP-4 protein in hindbrain; e, IGFBP-4 mRNA (*arrow*) in hindbrain.

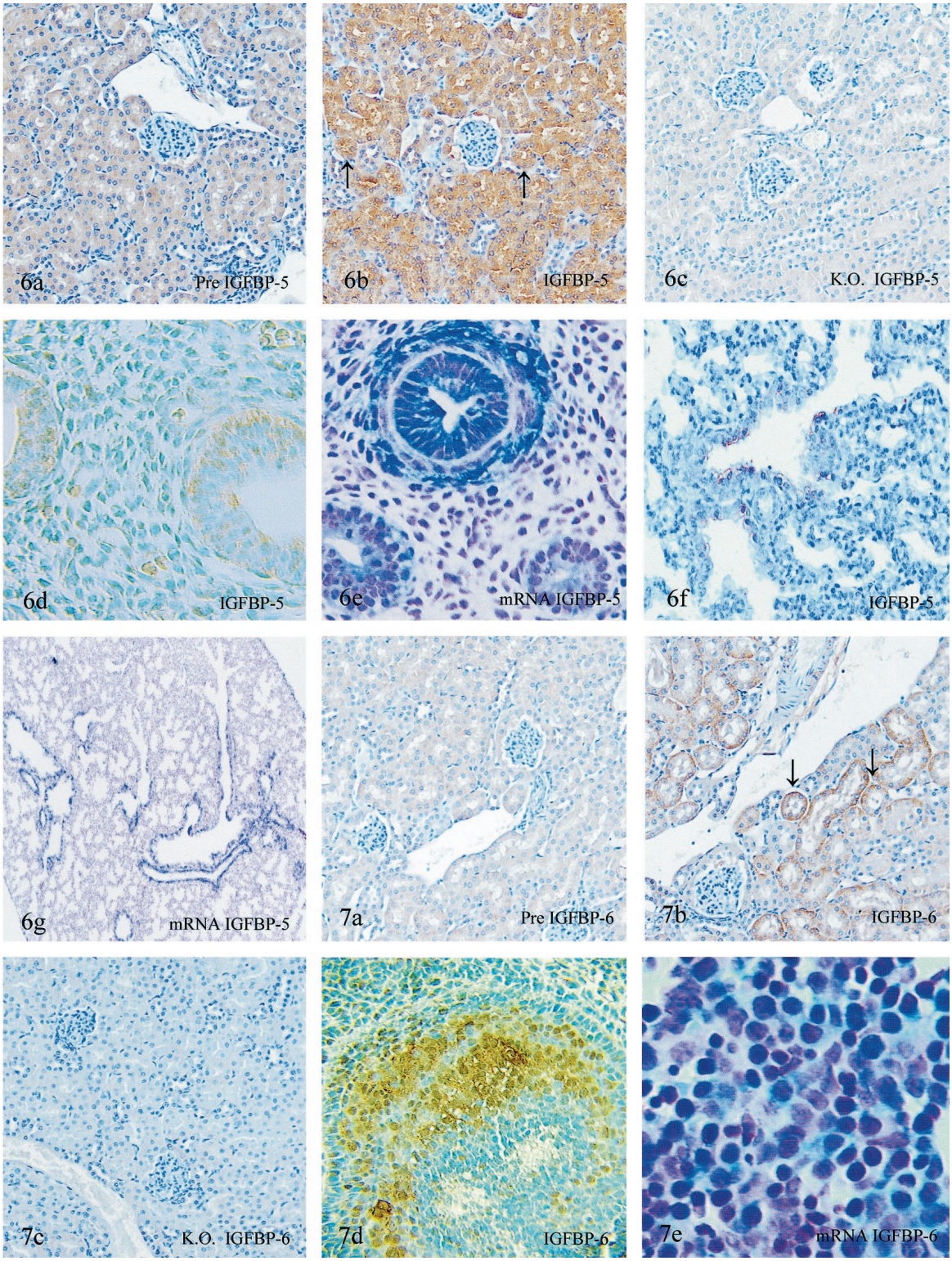

FIGS. 6–7. FIG. 6. Immunohistochemical detection of IGFBP-5 protein (*brown*) and IGFBP-5 mRNA (*blue*) in mouse adult kidney (a–c) and in 13.5-dpc embryonic lung (d and e) and 19.5-dpc embryonic lung (f and g). a, Kidney, preimmune serum (1:20) as a control for background staining; b, kidney, IGFBP-5 protein (*arrow*, IGFBP-5 protein in proximal tubules); c. kidney obtained from an IGFBP-5 gene deletion (K.O.) mutant, control for the specificity of the IGFBP-5 antiserum; d, IGFBP-5 protein in 13.5-dpc lung; e, IGFBP-5 mRNA in 13.5-dpc lung; f, IGFBP-5 protein in 19.5-dpc lung; g, IGFBP-5 mRNA in 19.5-dpc lung. FIG. 7. Immunohistochemical detection of IGFBP-6 protein (*brown*) and IGFBP-6 mRNA (*blue*) in mouse adult kidney (a–c) and in 13.5-dpc embryonic nasal epithelium (d) and liver (e). a, Kidney, preimmune serum (1:20) as a control for background staining; b, kidney, IGFBP-6 protein (*arrow*; IGFBP-6 protein in proximal tubules located around a vein); c, kidney obtained from an IGFBP-6 gene deletion (K.O.) mutant, control for the specificity of the IGFBP-6 antiserum; d, IGFBP-6 protein in the nasal epithelium; e, IGFBP-6 mRNA in liver.

TABLE 2. Localization of protein and mRNA of IGFBP-1 through -6 in major organs and tissues of the 13.5-dpc mouse embryo

	Protein	mRNA		Protein	mRNA
IGFBP-1	Liver	Liver	IGFBP-4	Mesencephalon	Mesencephalon
				Telencephalon	Telencephalon
IGFBP-2	Lung	Lung		Heart	Heart
	Liver	Liver		Liver	Liver
	Kidney	Kidney		Lung	Lung
	Choroid plexus	Choroid plexus		Tongue	Tongue
	Floor plate	Floor plate		Bloodvessels	Bloodvessels
				Kidney	
IGFBP-3	Liver	Liver			
	Tongue	Tongue	IGFBP-5	Liver	Liver
	Lung	Lung		Gut endothelium	Gut endothelium
	Nasal epithelium	Nasal epithelium		Meninges	Meninges
		Heart		Lung mesenchyme	Lung mesenchyme
	Choroid plexus			Tongue	Tongue
	Kidney			Notochord	
				Floor plate	
				Muscle	
			IGFBP-6	Liver	Liver
				Nasal epithelium	Nasal epithelium
					Perichondral
					Layers of cartilage
				Hindbrain	
				Heart	

tongue. In addition, protein was detected in the notochord, the floor plate, and muscle.

Colocalization of IGFBP-6 protein (Fig. 7d) and mRNA (weak, result not shown) was observed in nasal epithelium and in the liver (Fig. 7e). Protein was not detected in the perichondral layer of cartilage, as was found for mRNA. In addition, IGFBP-6 protein was visualized in hindbrain and the heart (results not shown).

Discussion

To analyze IGFBP protein localization in mouse embryonal tissues, we generated specific antisera against mIGFBP-1 through-6. The specificity of these antisera was demonstrated by ELISA, Western blotting (for IGFBP-1, -3, and -5), and immunohistochemistry on wild-type and IGFBP gene deletion mutants.

All antisera demonstrated specific staining patterns that were absent in preimmune controls and in tissues obtained from the corresponding gene deletion mutant. The fact that the antisera against mIGFBP-2, -4, and -6 were not able to detect the corresponding IGFBP on Western blot may be attributable to conformational changes of the protein induced by the Western-blot procedure.

Furthermore, immunohistochemical localization of mIGFBP proteins (mIGFBP-1 to -6) was compared with the mRNA patterns obtained with *in situ* hybridization of sections of the midgestational mouse embryo. These data extend our former gene expression studies that describe the tissue-specific mRNA expression of IGFBP-1 through -6 in the mouse embryo (15–17, 31, 32) and will be discussed.

Our results show that, similar to mRNA expression patterns, localization of IGFBP proteins in the mouse midgestational embryo is tissue-specific. IGFBP-1 mRNA and protein were detected primarily in the liver, whereas IGFBP-2, -4, and -5 were distributed among various tissues. Conform the low IGFBP-1, -3, and -6 mRNA levels, these IGFBPs were more difficult to detect than the other IGFBPs.

The limited data available on IGF system mRNA and protein expression during human development confirm our data (7–9, 33). IGFBP-2 expression is prominent during development of the nervous system, and the abundant IGFBP-2 protein and mRNA expression we observed in the choroid plexus confirmed previous observations (34, 35). In this respect, it is striking to note that we often observed a nuclear IGFBP-2 immunoreactivity in the embryological tissues. Although it is tempting to speculate about an intranuclear IGFBP-2 localization, such as described for IGFBP-3 (36), this cannot be concluded from these experiments.

Although protein localization of the IGFBPs seemed to be mostly similar to mRNA expression, some differences in localization in the 13.5-dpc mouse embryo were demonstrated.

Differences between IGFBP mRNA and protein localization may reveal detection thresholds for either mRNA or protein, or secretion of the protein without binding to the target organ (and protein is then probably washed out during the immunohistochemical procedure). Discrepancy between protein and mRNA expression was seen within tissues. In lung, IGFBP-2 mRNA was detected in epithelial cells of the tubules. However, IGFBP-2 protein was localized in the neighboring tubular cells. Similarly, IGFBP-3 mRNA and protein were located in neighboring cells in muscles of the tongue. Apparently, in these cases, mRNA expression in a given cell-type gives rise to protein localization in a cell-type that is in close contact. This may point to a mechanism of action where a certain cell type makes and secretes an IGFBP that acts at another (neighboring) cell-type.

Furthermore, substantial differences between mRNA and protein localization were found for IGFBP-3, -5, and -6. IGFBP-3 is the major circulatory IGFBP (1); and, after its

secretion in liver and the cardiovasculair system, IGFBP-3 can easily move throughout the embryo. The IGFBPs may be transported to specific sites, but the differences also may indicate that the mRNA is very labile in these specific tissues and, hence, present in concentrations below detection limits. In that case, translation should be efficient, and the protein must be very stable to enable protein detection.

Whereas mRNA and protein expression of the different IGFBPs was clearly distinct, most tissues were found to express more than one IGFBP. Examples are liver, lung, heart, and tongue. Two possible explanations for this phenomenon exist: all IGFBPs have a specific function and each contribution is necessary for a functional organ; or all IGFBPs have similar functions and show redundancy.

The fact that IGFBP knock-outs do not show dramatic phenotypes (14, 37) may suggest overlapping function or redundancy. The IGFBP-2 knock-outs are characterized by an decreased spleen size and changed IGFBP serum levels, probably to compensate for the lack of IGFBP-2 (37). The body weight and body length of the IGFBP-4 knock-outs are slightly smaller than of wild-type mice (14). However, these minor changes seen cannot be explained by changed patterns of IGFBP expression in tissues of interest.

The tissue-specificity of the IGFBPs and the consistence between IGFBP mRNA and protein localization patterns may suggest that the IGFBPs (except IGFBP-3) function in an autocrine or paracrine manner. The fact that several tissues express more than one IGFBP can also be explained as an indication for the complex regulation of the IGF system.

Summarizing, the generated antisera against mIGFBP-1 through -6 demonstrated specificity in ELISA, Western-blot, and immunohistochemistry. With these antisera, IGFBP protein localization could be compared with IGFBP mRNA expression patterns in 13.5-dpc mouse embryos. This revealed tissue-specific and consistent mRNA and protein localization, in confirmation with the suggested para- and autocrine functions of the IGFBPs on IGF action.

We anticipate that this set of specific antisera may become an important tool for future studies of IGFBP studies in the mouse.

Acknowledgments

We are very grateful to Dr. Ir. W. M. M. Schaaper, of the ID-DLO, for help with the design and generation of the synthetic peptides. Furthermore, S. Aupperlee has been of great help with technical assistance. We thank the Erasmus Dierexperimenteel Centrum (center for laboratory animal experiments) of the Erasmus University Rotterdam (EUR), the Netherlands, for the immunization of the rabbits. ^{125}I-IGF-II was kindly provided by Dr. S. van Buul-Offers, Wilhelmina Children's Hospital, Utrecht, the Netherlands. Prof. Dr. F. G. Grosveld (Department of Cell Biology and Genetics, EUR, The Netherlands) is thanked for the MEL cells. We also would like to thank Dr. R. Willemse (Department of Cell Biology, EUR, The Netherlands) and Dr. J. Laman (Department of Immunology, EUR, The Netherlands) for their helpful suggestions during the analysis of the antisera. Furthermore, we would like to thank Drs. T. Ludwig, A. Efstratiadis, K. Liu (Department of Genetics and Development, Columbia University, New York, NY) for their contributions in generating the IGFBP-3 KO mice; and Dr. P. Rotwein (Molecular Medicine Division, Oregon Health Sciences University, Portland, OR) for his contribution in generating the IGFBP-5 KO mutant mouse.

References

1. **Jones JI, Clemmons DR** 1995 Insulin-like growth factors and their binding proteins: biological actions. Endocr Rev 16:3–34
2. **Ludwig T, Eggenschwiler J, Fisher P, D'Ercole AJ, Davenport ML, Efstratiadis A** 1996 Mouse mutants lacking the type 2 IGF receptor (IGF2R) are rescued from perinatal lethality in *Igf2* and *Igf1r* null backgrounds. Dev Biol 177:517–535
3. **Liu J-P, Baker J, Perkins AS, Robertson EJ, Efstratiadis A** 1993 Mice carrying null mutations of the genes encoding insulin-like growth factor I (*Igf-1*) and the type I IGF receptor (*Igf1r*). Cell 75:59–72
4. **Liu ZZ, Wada J, Alvares K, Kumar A, Wallner EI, Kanwar YS** 1993 Distribution and relevance of insulin-like growth factor-I receptor in metanephric development. Kidney Int 44:1242–1250
5. **DeChiara TM, Efstratiadis A, Robertson EJ** 1990 A growth-deficiency phenotype in heterozygous mice carrying an insulin-like growth factor II gene disrupted by targeting. Nature 345:78–80
6. **Pannier EM, Irwin JC, Giudice LC** 1994 Insulin-like growth factor-binding proteins in the human fetus: tissue-specific protein secretion, immunologic characterization, and gene expression. Am J Obstet Gynecol 171:746–752
7. **Hill DJ, Clemmons DR** 1992 Similar distribution of insulin-like growth factor binding proteins-1, -2, -3 in human fetal tissues. Growth Factors 6:315–326
8. **Hill DJ, Clemmons DR, Riley SC, Bassett N, Challis JR** 1989 Immunological distribution of one form of insulin-like growth factor (IGF)-binding protein and IGF peptides in human fetal tissues. J Mol Endocrinol 2:31–38
9. **Han VK, Hill DJ, Strain AJ, Towle AC, Lauder JM, Underwood LE, D'Ercole AJ** 1987 Identification of somatomedin/insulin-like growth factor immunoreactive cells in the human fetus. Pediatr Res 22:245–249
10. **van Kleffens M, Groffen C, Lindenbergh-Kortleve DJ, van Neck JW, González-Parra S, Dits N, Zwarthoff EC, Drop SLS** 1998 The IGF system during fetal-placental development of the mouse. Mol Cell Endocrinol 140:129–135
11. **Adesanya OO, Zhou J, Samathanam C, Powell-Braxton L, Bondy CA** 1998 IGF-I and uterine growth. In: Takano K, Hizuka N, Takahashi S-I (eds) Molecular Mechanisms to Regulate the Activities of Insulin-Like Growth Factors. Elsevier Science, Amsterdam, the Netherlands, pp 163–168
12. **Erickson GF, Kubo T, Li D, Kim H, Shimasaki S** 1998 The IGF system in the ovary. In: Takano K, Hizuka N, Takahashi S-I (eds) Molecular Mechanisms to Regulate the Activities of Insulin-Like Growth Factors. Elsevier Science, Amsterdam, the Netherlands, pp 185–194
13. **Hill DJ, Petrik J, Arany E, Reik W, Pell JM** 1998 Insulin-like growth factors in the development of the pancreas. In: Takano K, Hizuka N, Takahashi S-I (eds) Molecular Mechanisms to Regulate the Activities of Insulin-Like Growth Factors. Elsevier Science, Amsterdam, the Netherlands, pp 145–154
14. **Pintar JE, Schuller A, Bradshaw S, Cerro J, Grewal A** 1998 Genetic disruption of IGF binding proteins. In: Takano K, Hizuka N, Takahashi S-I (eds) Molecular Mechanisms to Regulate the Activities of Insulin-Like Growth Factors. Elsevier Science, Amsterdam, the Netherlands, pp 65–70
15. **van Kleffens M, Groffen C, Rosato RR, van den Eijnde SM, van Neck JW, Lindenbergh-Kortleve DJ, Zwarthoff EC, Drop SLS** 1998 mRNA expression patterns of the IGF system during mouse limb bud development, determined by whole mount in situ hybridization. Mol Cell Endocrinol 138:151–161
16. **Lindenbergh-Kortleve DJ, Rosato RR, van Neck JW, Nauta J, van Kleffens M, Groffen C, Zwarthoff EC, Drop SLS** 1997 Gene expression of the insulin-like growth factor system during mouse kidney development. Mol Cell Endocrinol 132:81–91
17. **Schuller AGP, van Neck JW, Lindenbergh-Kortleve DJ, Groffen C, de Jong I, Zwarthoff EC, Drop SLS** 1994 Gene expression of the IGF binding proteins during post-implantation embryogenesis of the mouse; comparison with the expression of IGF-I and -II and their receptors in rodent and human. In: LeRoith D, Raizada MK (eds) Current Directions in Insulin-Like Growth Factor Research. Plenum Press, New York, pp 267–277
18. **Green BN, Jones SB, Streck RD, Wood TL, Rotwein P, Pintar JE** 1994 Distinct expression patterns of insulin-like growth factor binding proteins 2 and 5 during fetal and postnatal development. Endocrinology 134:954–962
19. **Cerro JA, Grewal A, Wood TL, Pintar JE** 1993 Tissue-specific expression of the insulin-like growth factor binding protein (IGFBP) mRNAs in mouse and rat development. Regul Pept 48:189–198
20. **Wood TL, Streck RD, Pintar JE** 1992 Expression of the IGFBP-2 gene in post-implantation rat embryos. Development 114:59–66
21. **Liu X-J, Malkowski M, Guo Y, Erickson GF, Shimasaki S, Ling N** 1993 Development of specific antibodies to rat insulin-like growth factor-binding proteins (IGFBP-2 to -6): analysis of IGFBP production by rat granulosa cells. Endocrinology 132:1176–1183
22. **Kyte J, Doolittle RF** 1982 A simple method for displaying the hydropathic character of a protein. J Mol Biol 157:105–132
23. **Fasman GD, Chou PY** 1976 Prediction of protein conformation: consequences and aspirations. In: Blout ER (ed) Peptides, Polypeptides and Proteins, New York, Wiley, pp 114–125

24. **Jameson BA, Wolf H** 1988 The antigenic index: a novel algorithm for predicting antigenic determinants. Comput Appl Biosci 4:181–186
25. **Needham M, Gooding C, Hudson K, Antoniou M, Grosveld F, Hollis M** 1992 LCR/MEL: a versatile system for high-level expression of heterologous proteins in erythroid cells. Nucleic Acids Res 20:997–1003
26. **Hossenlopp P, Seurin D, Segovia-Quinson B, Hardouin S, Binoux M** 1986 Analysis of serum insulin-like growth factor binding proteins using Western blotting: use of the method for titration of the binding proteins and competitive binding studies. Anal Biochem 154:138–143
27. **Wood TL, Rogler L, Streck RD, Cerro J, Green B, Grewal A, Pintar JE** 1993 Targeted disruption of IGFBP-2 gene. Growth Regul 3:5–8
28. **Schuller AGP, Pintar JE** Embryonic growth deficit in IGFBP-4 deficient mice. Program of the 80th Annual Meeting of The Endocrine Society, New Orleans, 1998, p 59 (Abstract)
29. **Schuller AGP, Bradshaw SL, Green BN, Rotwein PS, Pintar JE** Targeted disruption of the mouse IGFBP-5 gene. Program of the 81st Annual Meeting of The Endocrine Society, San Diego, 1999, p 83 (Abstract)
30. **Bradshaw SL, Grewal A, Pintar JE** Determination of a developmental role for insulin-like growth factor binding protein-6. Program of the 4th International Symposium on Insulin-Like Growth Factors, Tokyo, 1997, p 57 (Abstract)
31. **Schuller AGP, van Neck JW, Beukenholdt RW, Zwarthoff EC, Drop SLS** 1995 IGF, type I IGF receptor and IGF-binding protein mRNA expression in the developing mouse lung. J Mol Endocrinol 14:349–355
32. **Schuller AGP, Zwarthoff EC, Drop SLS** 1993 Gene expression of the six insulin-like growth factor binding proteins (IGFBPs) in the mouse conceptus during mid- and late-gestation. Endocrinology 132:2544–2550
33. **Han VK, Matsell DG, Delhanty PJ, Hill DJ, Shimasaki S, Nygard K** 1996 IGF-binding protein mRNAs in the human fetus: tissue and cellular distribution of developmental expression. Horm Res 45:160–166
34. **Wood TL, Brown AL, Rechler MM, Pintar JE** 1990 The expression pattern of an insulin-like growth factor (IGF)-binding protein gene is distinct from IGF-II in the midgestational rat embryo. Mol Endocrinol 4:1257–1263
35. **Sullivan KA, Feldman EL** 1994 Immunohistochemical localization of insulin-like growth factor-II (IGF-II) and IGF-binding protein-2 during development in the rat brain. Endocrinology 135:540–546
36. **Jaques G, Noll K, Wegmann B, Witten S, Kogan E, Radulescu RT, Havemann K** 1997 Nuclear localization of insulin-like growth factor binding protein 3 in a lung cancer cell line. Endocrinology 138:1767–1770
37. **Pintar JE, Schuller A, Cerro JA, Czick M, Grewal A, Green B** 1995 Genetic ablation of IGFBP-2 suggests functional redundancy in the IGFBP family. Prog Growth Factor Res 6:437–445